Modified Cole–Cole Plot Based on Viscoelastic Properties for Characterizing Molecular Architecture of Elastomers*

E. R. HARRELL and N. NAKAJIMA, *B. F. Goodrich Chemical Group, Technical Center, P.O. Box 122, Avon Lake, Ohio 44012*

Synopsis

The types of molecular architecture commonly present in many commercial elastomers include long branching, which in extreme cases results in crosslinked gel network. This architecture was modeled by preparing a series of ethylene–propylene copolymer samples in which the degree of branching was systematically varied. The frequency-dependent viscoelastic properties of these model systems were measured over a temperature range of 80–230°C with a Rheometrics Mechanical Spectrometer. Time–temperature superposition was employed to obtain master curves of the storage G' and loss G'' moduli and complex viscosity. The viscoelastic properties of the model samples change systematically with the variations in molecular architecture. Specifically, the low frequency Newtonian viscosity behavior is progressively replaced by non-Newtonian power-law behavior, and the G' response relative to that of the G'' is significantly enhanced as long-branching increases. The practical use of a modified Cole–Cole plot, in which the axes are expressed as the logarithms of G' and G'', for analysis of molecular architecture is demonstrated. Changes in the long-branch architecture of the model samples were readily detected as systematic variations in shape and displacement of the modified Cole–Cole plot. On the other hand, the data of molecularly linear elastomer samples of different M_w but similar MWDs were reduced to a single master Cole–Cole plot.

INTRODUCTION

Since the time when synthetic elastomers first became available, the presence of a specific molecular architecture has been recognized to be of practical importance. Elastomers produced under certain conditions were found to be difficult to process on the mill, i.e., behaving as if they contained crosslinked structure. These elastomers were often, but not always, found to contain "gels," i.e., fractions insoluble but swellable in solvents. Examination of the polymerization conditions, and of post-polymerization treatment such as drying, readily indicated the occurrence of chain-coupling reactions, which led to formation of long-chain branching and gel network.

Characterization of the above molecular architecture as well as an average molecular weight and molecular weight distribution has been recognized to be important in support of both production and processing of elastomers. A knowledge of these molecular parameters provides criteria for controlling polymerization and other production conditions, thereby assuring consistently good product quality. The processing of elastomers also requires knowledge

* Presented at the ACS Symposium on Effects of Molecular Structure on the Rheology of Flexible and Rodlike Polymers, Kansas City, Kansas, September 13–15, 1982.

Journal of Applied Polymer Science, Vol. 29, 995–1010 (1984)
 CCC 0021-8995/84/030995-16$04.00

of these molecular properties, because they determine the rheological behavior and, hence, processability during mixing and forming operations.

A large number of experimental techniques have been employed to measure the various molecular parameters, such as number average molecular weight (M_n), weight average molecular weight (M_w), molecular weight distribution (MWD), and "degree of branching." These techniques include light scattering, osmometry, gel permeation chromatography, sedimentation, and dilute solution viscometry.[1] Each relies upon the complete solubility of a polymer in an appropriate solvent for assurance of measurement accuracy. Although all of these techniques have been extensively employed for characterization of elastomers, uncertainties in the validity of the measurement often arise due to the limited solubility of the high molecular weight and/or branched species typically present in commercial elastomers. Additionally, solution based techniques are generally too time-consuming for use in routine quality control measurements.

In order to circumvent some of the difficulties encountered in solution measurements, an alternate approach has evolved for quality control and processability evaluation which is based upon characterizing the manifestations of the molecular parameters in the rheological behavior of polymer melts. This approach has been examined in great detail in academia as well as within the polymer industry.[2]

For example, instead of M_w, the low shear Newtonian viscosity η_0, may be used as a key parameter, if the sample is a linear polymer and its MWD is narrow:

$$\eta_0 = KM_w^{3.4} \quad \text{for } M_w > M_c \tag{1}$$

where M_c is a characteristic molecular weight above which chain entanglement becomes important.[3]

However, this method is not applicable to most of the commercial elastomers, since the presence of a high molecular weight fraction requires prohibitively low deformation rates for measuring the terminal flow response.

Kraus and Gruver[4] suggested that a molecular weight shift factor α_m may be substituted for η_0 in eq. (1):

$$\alpha_m = K'M_w^{3.4} \tag{2}$$

The shift factor α_m corresponds to the amount of shift required to superpose the viscosity–shear rate data, η ($\dot{\gamma}$), of a polymer sample onto a viscosity master curve in a procedure analogous to the time–temperature shift.[5] This presupposes that the η ($\dot{\gamma}$) curves of polymers have the same shape; this sets a limitation that there is no significant variation in MWD or in the degree of branching among the samples being compared.

The shear-rate-dependent viscosity of polymer melts has also been employed to examine differences in MWD for systems of similar M_w and molecular architecture. The analysis of MWD is based upon the concept that the low shear rate viscosity reveals relaxation processes of the larger molecules whereas the high shear rate viscosity is dominated by relaxation processes associated with the smaller molecules and segments of larger molecules.[6] Thus differences in the magnitudes and shapes of the η ($\dot{\gamma}$) curves are indirect but quantitative expressions for MWD. Studies of polyethylene indicate that the low shear rate viscosities of broad MWD samples are higher than those of narrow MWD samples. However, the high shear rate viscosity decreases as MWD increases, leading to crossovers in the η ($\dot{\gamma}$) curves for samples of varying MWD.[7,8] Similar results

were obtained for polystyrene. In this study[9] a monodispersed sample was compared with a polydispersed polystyrene of similar M_w. Two crossovers in the η ($\dot{\gamma}$) curves were observed. At low and very high shear rates the viscosity of the broad MWD sample was higher than that of the narrow MWD sample. The relationship was reversed at intermediate shear rates. Changes in MWD have also been detected by melt recovery[8] and entrance and exit pressure loss[10] measurements using capillary rheometers. Sometimes, the broadening of MWD is accompanied by increases in melt recovery or die swell and increases in entrance and exit pressure losses. In general, however, the MWD dependence of these parameters is very complex; they are not simple functions of average molecular weights or their ratios.

Elucidation of the effects of molecular branching upon the melt viscosity of polymers has been problematic, partly because of the difficulty in defining in a quantitative manner the variations in the types and distributions of branches existing in most commercial polymers.[11] Another difficulty is the separation of MWD effects from those of branching. In order to circumvent some of these difficulties, researchers have prepared and examined a variety of model systems in which the number of branches per molecule, the branch length and the molecular weight are precisely controlled. These model systems include star molecules,[12,13] comb molecules,[14] and randomly branched molecules.[15]

Kraus and Gruver[16] were the first to quantitatively describe the relationship between branch architecture and the shear rate dependent viscosity of polybutadiene. The major feature of this relationship is that the low shear rate Newtonian viscosity η_0 of a polymer having branches of molecular weight M_b less than 3–4 times M_c is less than that of a linear polymer of similar M_w. For cases in which M_b of the branches system exceeds 3–4 times M_c, then η_0 of the branched polymer exceeds that of the linear polymer—later described as η_0 enhancement.[13] A further observation was that the high shear rate non-Newtonian viscosities of the branched systems were lower than those of the linear counterparts, even though viscosity enhancement was observed at low shear rates. Thus the mechanisms for viscosity enhancement must be shear rate dependent. The concept of a shear rate dependent M_c and its use in rheological models and for the classification of "long" and "short" branches have been discussed elsewhere.[11]

The recent extensive work of Graessley and co-workers[13,17,18] with monodispersed linear and star polybutadienes and their hydrogenated products supports the earlier observations by Kraus and Gruver. However, the η_0 enhancement was compared at equal hydrodynamic volume instead of equal molecular weight.

Methods other than the characterization of η ($\dot{\gamma}$) have been employed to examine differences in the molecular architecture of polymers. Differences in the large deformation response of elastomers have been ascribed to variations in molecular branching. The presence of long branches in butadiene–acrylonitrile copolymer produces strain hardening.[19,20]

Melt elasticity, as manifested in die swell[21] and pressure losses in the entrance and exit regions of capillary flow geometries,[10] has been found to significantly increase with degree of branching. However, in general the melt elasticity is not a simple function of the degree of branching. It varies with shear rate and the shear-rate dependence is affected in a complex manner by branch length and degree of branching.

The concentration dependence of viscoelastic properties was shown to be significantly affected by the presence of long branches.[22,23] The long-branch polymer not only produced different shift factors in the concentration superposition but also deviated from the master curve at semidilute concentrations.[23]

Folt[24] observed that the relative degree of long chain branching in polybutadiene and polyisoprene could be assessed by the magnitude of stress oscillation encountered in capillary flow measurements: the magnitude of the stress oscillation decreased with increasing long chain branching. Folt[25] also recognized that linear chains possess a distinct plateau region of behavior which is dominated by the storage modulus (G') at high frequencies. At low frequencies, linear chains display near-terminal flow behavior which is dominated by the loss modulus (G''). However, the frequency-dependent viscoelastic properties of polymers containing long branches are dominated by the G' response even at low frequencies, revealing no G'–G'' crossover.

For further investigation of the use of viscoelastic measurements for the assessment of the molecular architecture of elastomers, EPM model samples, systematically different in degree of branching, were prepared and characterized. The details and results of this study are the subjects of this paper.

EXPERIMENTAL

Sample Preparation

An experimental ethylene–propylene copolymer, EPM, containing 54 wt % ethylene, designated as XL-0, was selected as the base elastomer. It is an amorphous, relatively low molecular weight elastomer. The conditions and method of polymerization are designed to make the XL-0 copolymer free of branches. The molecular architecture of the model samples was varied by inducing partial crosslinking with dicumyl peroxide in the high shear environment of a Banbury mixer. The sample designation and the variation in amounts of dicumyl peroxide used in sample preparation are shown in Table I. All samples with the exception of XL-0 were prepared as follows:

1. The dicumyl peroxide was dispersed in the base elastomer first by banding the EPM on a warm mill (approximately 80°C) for five passes with the mill rolls relatively open. The dicumyl peroxide was then spread uniformly across the elastomer sheet after which an additional five passes on a tight mill were used

TABLE I
Sample Description

Designation	Dicumyl peroxide level (phr)[a]	Final batch temp (°C)[b]
XL-0	0.0	—
XL-1	0.05	188
XL-2	0.1	199
XL-3	0.2	193
XL-4	0.4	179

[a] phr = parts per hundred parts of rubber by weight.

[b] Temperature as measured by the Banbury thermocouple. Actual batch temperature may be somewhat higher.[26]

for dispersion. Each pass was followed by a rolling and folding of the elastomer sheet.

2. The samples were then masticated in a size B Banbury mixer at slow speed (77 rpm) with steam applied to the rotor and chamber walls until the batch thermocouple indicated 150°C. Mastication was continued for an additional three minutes without the use of steam. Final batch temperatures were measured and are presented in Table I.

3. Following the mastication, the samples were passed through a warm mill to form sheets and were allowed to cool to room temperature.

Actual temperatures attained by the samples during mastication were probably 15–20° higher than those reported in Table I.[26] Based upon cure-time date for this system,[27] reaction should be complete within 1 min at 200°C and three minutes at 190°C. It was anticipated (and verified by viscoelastic measurements) that the above thermal history was sufficient to provide for complete reaction of the dicumyl peroxide.

Instrument Operation

A high temperature gel permeation chromatograph (Waters Associate Model 200) containing five styragel packed columns of pore size ranging from 10^2 to 10^6 Å was used to measure the molecular size distributions of the samples. The polystyrene equivalent hydrodynamic volume measurements were converted to EPM molecular weight through the use of a Q factor for linear EPM. No corrections were made for the effects of branching. Solution preparation and GPC measurements were performed with trichlorobenzene at 135°C. Prior to injecting into the GPC columns, the sample solutions were filtered through an HAKI Krueger filter having a pore size of approximately 0.1 μm.

The melt viscoelastic properties of the XL samples were measured with a Rheometrics Mechanical Spectrometer using the oscillating parallel plate mode at 80°C, 125°C, and 230°C over the angular frequency range of 10^{-1}–10^2 s^{-1}. Strain amplitudes of 0.02, 0.05, and 0.12 were used at temperatures of 80°C, 125°C, and 230°C. Sample response linearity with respect to strain amplitude was verified at each test condition. The larger strain amplitudes were required at high temperatures to improve instrument signal resolution at low frequencies. At the conclusion of each test the viscoelastic properties of the samples were remeasured at selected high and low frequencies to examine sample stability. These data agreed within 5% of the initial measurements for the 230°C data and within 2% of those obtained at temperatures lower than 230°C. In addition to assuring sample stability, these data indicate that the dicumyl-peroxide-induced reactions were completed during sample preparation.

RESULTS

GPC Measurements

The branched XL samples, prepared as previously described, are not as amenable to exact description of their molecular parameters as other model systems referenced in the introduction, because of the generation of multiple structures and alteration of MWD. Peroxide induced reactions can produce chain-scission molecular fragments, with accompanying double bond formation,

and crosslinks consisting of di-, tri-, and tetrafunctional bond formation.[28] Thus peroxide reactions can: (1) lower M_w by scission reactions; (2) increase M_w of linear molecules by end coupling; (3) increase M_w and produce branching via tri- and tetra-branch formation; and (4) produce a chemical network (gel) via (3) above, if the concentration of the reactant species is sufficiently high. Further complications may arise from oxidation, shear, and thermally induced reactions in the Banbury mixer.[29] The rationale for using the Banbury mixer was that the high shear stresses encountered during Banbury mastication tend to selectively break down the high molecular weight species, thereby offsetting the tendency to produce samples containing broad MWD and macroscopic gel domains.

The difficulties in determing molecular parameters, especially with respect to branch structure, for the XL samples as described above is typical of the situation encountered with many commercial polymers. Often, differences among commercial samples are much smaller than the differences among the XL samples. For this reason GPC analyses have not been very useful when the complexity of branch architecture is involved. In the present study the XL samples were prepared to exaggerate the differences. Even so, we do not intend to use GPC data for an extensive analysis of the molecular structures, because the result will not be applicable to practical situations in which samples possess only small differences. Rather an objective of our work is to demonstrate that viscoelastic data furnish quantitative, although relative, information of practical importance on the molecular parameters discussed above.

The GPC data are presented here to provide relative information on the branch formation and chain scission as described below. The symbols M_z, M_w and M_n are used here and in later discussions to describe relative hydrodynamic size only and, as such, do not differentiate linear from branched chains.

The results from the GPC analysis of the XL samples are tabulated in Table II. Inspection of the normalized GPC curves (Fig. 1) reveals that the lower peroxide concentrations used in the preparation of XL-1 and XL-2 did not produce many large hydrodynamic size species or substantially change the hydrodynamic size distribution as described by the curve shapes and tabulated M_w/M_n values. A slight shift of the total distribution towards lower molecular hydrodynamic size as peroxide concentration is increased is observed. This shift is attributable to the formation of progressively larger amounts of molecular branching and chain scission during Banbury mixing. Because the GPC data

TABLE II
GPC Measurements of XL Series[a]

Sample	Dicumyl peroxide (phr)	M_n (10^4)	M_w (10^5)	M_z (10^5)	M_w/M_n	M_v (10^5)	DSV[b]
XL-0	0.0	5.37	1.16	2.87	2.16	1.04	1.45
XL-1	0.05	4.96	1.04	2.31	2.10	0.94	1.40
XL-2	0.1	4.34	0.96	2.34	2.22	0.86	1.33
XL-3	0.2	4.52	1.18	4.33	2.61	1.02	1.38
XL-4	0.4	4.53	2.37	41.57	5.23	1.64	1.67

[a] Symbols M_n, M_w, M_z, and M_v describe relative hydrodynamic size, i.e., molecular weight averages are not corrected for branching.

[b] Dilute solution viscosity determined with a concentration of 0.1 g/dL in toluene at 25°C.

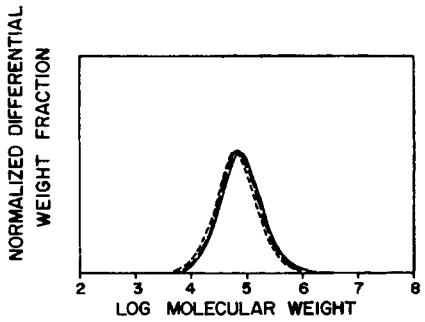

Fig. 1. Variation in molecular weight distribution of branched EPM samples for low level addition of dicumyl peroxide. (—) XL-0; (– –) XL-1; (- - -) XL-2.

are uncorrected for branching but are hydrodynamically equivalent to the molecular weight of linear polymer, the exact nature of the branch formation and absolute quantification of molecular weight averages are masked in these data.

The effect of adding higher concentrations of dicumyl peroxide is displayed in the GPC curves of XL-3 and XL-4 (Fig. 2). As shown the curves indicate that progressively more species of large molecular hydrodynamic size were formed as the concentration of peroxide was increased from 0.1 to 0.4 phr, leading to the development of apparently large hydrodynamic size tails and broader distribution. An interesting point to note in Table II is the relative insensitivity of M_n to an increase in peroxide addition, whereas M_z values increase dramatically at peroxide addition in excess of 0.1 phr. Figure 3 is included for the purpose of illustrating the extremes in hydrodynamic size distribution covered by the series of model samples.

In addition to characterization with GPC, dilute solution viscosity (DSV) measurements were obtained for the samples. These results are also reported in Table II. As part of the procedures of both the DSV and GPC analysis, gel determinations were performed. The DSV method of gel determination incorporated a coarse filter which eliminates macroscopic gels. No macroscopic gels were detected in any of the samples. The GPC method uses an instrument response factor (actual area under the chromatograms/expected area for a given solution concentration) and thus should be an estimate of gel particles retained by the 0.1 μm filter. The gel measurements suggest that XL-4 was the only case in which microgels were formed as the result of peroxide addition (ca. 14%).

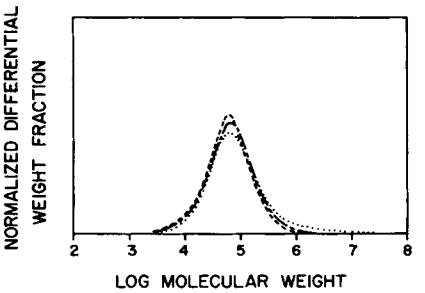

Fig. 2. Variation in molecular weight distribution of branched EPM samples for high level additions of dicumyl peroxide. (- - -) XL-2; (— - —) XL-3; (· · ·) XL-4.

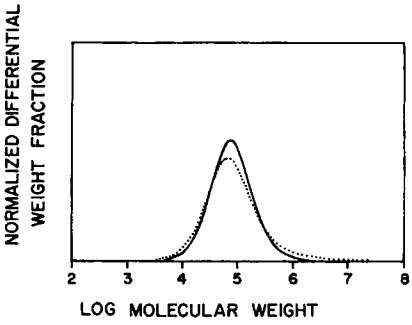

Fig. 3. Comparison of the molecular weight distribution for the linear, XL-0 (—), and most highly branched, XL-4 (···), samples.

Viscoelastic Property Measurements

The measurements of storage modulus G', loss modulus G'', and complex viscosity $|\eta^*|$ obtained at 80°C, 125°C, and 230°C were reduced to master curves at 230°C for each sample through the application of time–temperature superposition. The density and temperature correction, $T_0\rho_0/T\rho$, where the subscripted variables refer to conditions at 230°C was not required to obtain the best superposition among both G' and G'' data for any of the samples except XL-0. For the XL-0 sample, small vertical shifts of 0.9 and 0.84 were needed for superposition of the 125°C and 80°C measurements, instead of the calculated values of 1.19 and 1.31, respectively. Others[30] have also noted cases in which the form of the above density and temperature correction is inappropriate and have offered possible explanations.

Exact superposition was not obtained for the G' and G'' data of XL-4. The deviation was such that at the lower frequencies a larger temperature dependence was observed. A similar temperature dependence was observed by Sabia with the steady state viscosity of low density polyethylene.[31] This suggested that time–temperature superposition is not applicable to elastomers containing a large amount of long branching. Graessley and co-workers[17,18] found similar difficulty in applying time–temperature superposition with hydrogenated products of star branched polybutadiene. For purposes of comparing the effects of progressive changes in molecular architecture, an approximate master curve was constructed for XL-4 in which the 230°C reference temperature data were weighted more heavily than the others. The degree of approximation used for the XL-4 master curve does not alter the observations and conclusions contained in the following discussion.

The $|\eta^*|$ (ω) master curves of the various samples are compared in Figure 4, where the effect of branch formation with various amounts of dicumyl peroxide are shown. The XL-0 sample displays two distinct regions of behavior; the approach of Newtonian behavior at low frequencies and the nearly power-law behavior at high frequencies. As the amount of long branching increases, the $|\eta^*|$ in the low frequency region increases and the $|\eta^*|$ in the high frequency region decreases. The most significant observation is that the response approaching Newtonian behavior is progressively replaced by non-Newtonian, power-law behavior with increases in the degree of long branching.

Although none of the samples display a η_0 within the observe frequency range, $|\eta^*|$ values at low frequencies are assumed to reflect the relative differences in

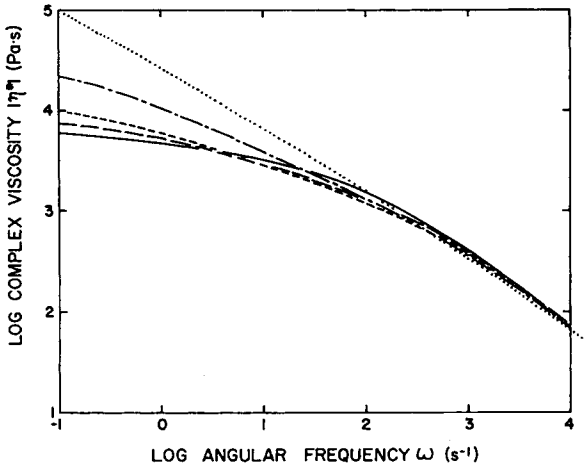

Fig. 4. Effect of increasing long branching (XL-0–XL-4) on the complex viscosity master curves at 230°C. (—) XL-0; (– –) XL-1; (– · –) XL-2; (— · · —) XL-3; (· · ·) XL-4.

their respective η_0. The differences in magnitudes of the viscosities at 10^{-1} s^{-1} of XL-0, XL-1, and XL-2 suggest a progressive increase in η_0 enhancement as the degree of long branching is increased, regardless whether a constant M_w or constant DSV based comparison is used (refer to Table II). Furthermore, the types of branch structures formed during sample preparation can be described as possessing M_b >3–4 times M_c[16–18] for this polymer system.

The G' and G'' master curves for XL-0, XL-1, and XL-2 are shown in Figure 5. As was observed in the viscosity data, significant differences in frequency dependent behavior exist among the samples. However, the nature of the differences is more readily recognized. Sample XL-0 possesses two well-defined regions of response; the high frequency region is dominated by the G' response, characteristic of the approaching rubber plateau, and the low frequency region is dominated by the G'' response which is approaching a slope of 1, characteristic of terminal flow.

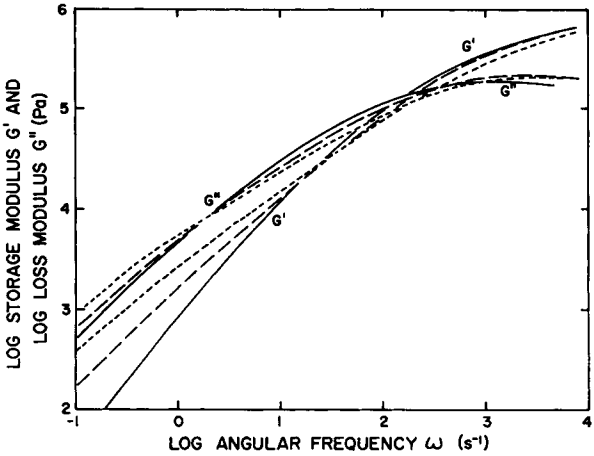

Fig. 5. Systematic changes in the low frequency contributions of G' and G'' with increasing levels of long branching; XL-0 through XL-2. Master curves referenced at 230°C. (—) XL-0; (– –) XL-1; (– · –) XL-2.

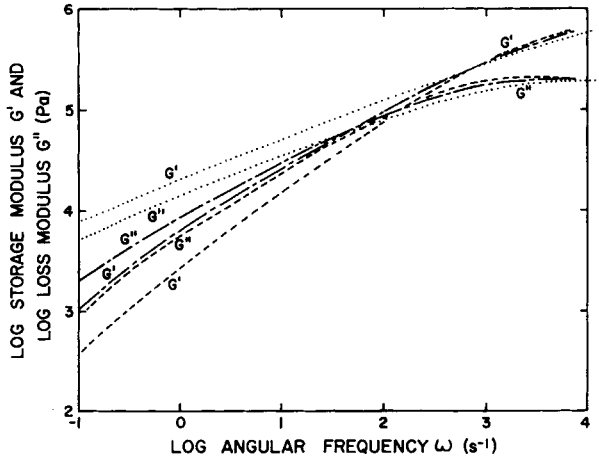

Fig. 6. Systematic changes in the G' and G'' master curves at 230°C with increasing levels of long branching; XL-2, through XL-4. (- - -) XL-2; (— - —) XL-3; (· · ·) XL-4.

Examination of the low frequency region reveals that the contribution of the G' to the total response increases as degree of branching increases. More specifically, increases in the degree of long branching provides additional long-time relaxation mechanisms, thereby broadening the relaxation spectrum.

The progressive increase of the low frequency storage modulus with the further increase in long branching is shown by the data of samples XL-3 and XL-4 (Fig. 6). For the most extreme case, XL-4, the G' response dominates over the entire range of observed frequencies; i.e., no G'–G'' crossover was observed.

In addition to the noted changes in the low frequency behavior, the characteristic features in approaching the rubbery plateau change; the G'' maximum and the region of low $\partial \ln G'/\partial \ln \omega$ seem to shift to higher frequencies as degree of long branching increases. Figure 7 illustrates the extremes in the types of viscoelastic behavior associated with the linear and most extensively branched sample.

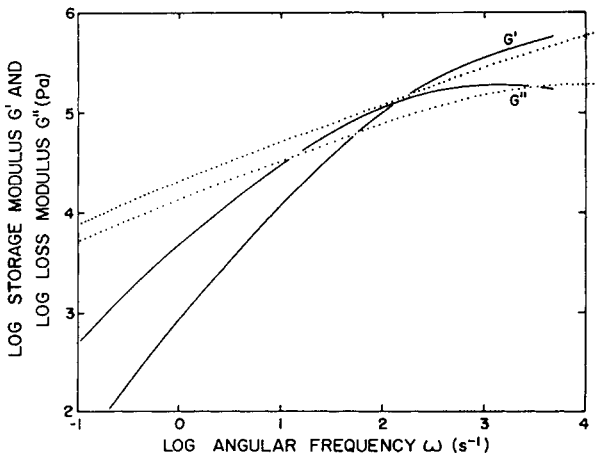

Fig. 7. Comparison of the G' and G'' master curves at 230°C for the linear, XL-0 (——), and most extensively branched, XL-4 (· · ·), samples.

These results can be contrasted with those obtained by others from studies of linear and star-branched polystyrene[12] and polybutadiene.[13] Those model polymer systems each displayed well-defined terminal flow regions of behavior in which G' and G'', were proportional to ω to the second and first power, respectively. This permitted measurement of Newtonian viscosities, even for the star-branched polymers of high molecular weight. These features were unattainable for the model samples of this study. The enhancement of η_0 and broadening of the relaxation spectrum resulting from the introduction of branching were also previously noted. However, the accompanying change in the G' contribution relative to that of the G'' was not so apparent.

The variations in behavioral characteristics of previous model systems relative to those presented in this study are attributed to two differences within the model systems. Previous systems were nearly monodispersed and contained only star-branched structures. The polydispersity of the base polymer used in the present study is typical of commercial EPM elastomers. Additionally, based upon observed viscoelastic behavior of commercial EPDM elastomers,[23,32] the types of branch structures formed in the XL samples are representative of those present in commercial elastomers.

A better method of comparing the differences in viscoelastic behavior resulting from variations in long branching is to contrast G'' against G'. For this purpose the Cole–Cole plot[33,34] mode of presentation was modified by using as the axes the logarithms of G'' and G', as shown in Figure 8. Each point on the curve represents a different reduced angular frequency. This form of data presentation is a mapping of the relative contribution of the G'' response to that of G'.

The linear Cole–Cole plot, originally formulated to analyze and represent complex dielectric constant data in terms of simple, discrete relaxation mechanisms, has been adapted by others[35,36] to perform similar analysis of complex compliance data. However, our present use of the modified, logarithmic Cole–Cole plot is as an empirical tool which sensitively resolves variations in the branch structure of polymers. The ramifications of this attribute is the subject of future studies.

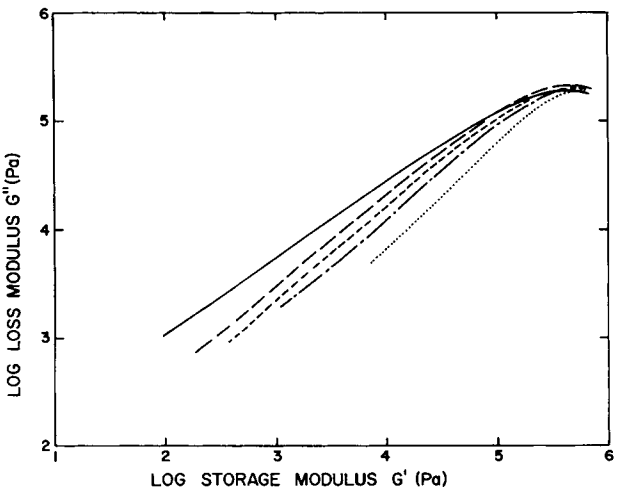

Fig. 8. Modified Cole–Cole plot showing G' enhancement as degree of long branching increases: XL-0 through XL-4. (—) XL-0; (– –) XL-1; (– – –) XL-2; (— – —) XL-3; (· · ·) XL-4.

The modified Cole–Cole plot of the unbranched XL-0 sample reveals several features. The region of the maximum in the curve corresponds to the rubber plateau region of behavior. The terminal flow region should be depicted as a low moduli region over which G'' is proportional to G' to the 0.5 power. This type of behavior is approached but not well-defined for the XL-0 sample. Instead, the Cole–Cole plot of XL-0 shows a rather broad transition from rubber plateau behavior to the onset of terminal flow behavior which covers several decades of moduli values. The presence of this broad transition region is attributed to the polydispersity of molecular size of the XL-0 sample.

The increase of the G' value with increasing degree of long branching is readily apparent by the progressive displacement of the respective Cole–Cole plots from XL-0 to XL-4. The fact that long branching tends to shift the low frequency behavior away from the terminal flow response is indicated by the change in the slope of the low moduli region to values much larger than the Newtonian slope of 0.5.

As discussed previously, an approximation was made to obtain the XL-4 master curve. The extent of approximation is shown in Figure 9 which contains the data obtained at each of the three temperatures. Lack of superposition is not attributable to the omission of the $T_0\rho_0/T\rho$ factor, because its inclusion would result in a diagonal equimoduli shift which would not provide a better superposition. These data suggest that for highly branched systems, higher temperatures make the G' and G'' responses more similar to those of linear molecules. This may be interpreted as a decrease in the amount of branch entanglement or constraints at branch points.

There is an additional feature of the Cole–Cole plot which warrants comment. Viscoelastic data plotted in this manner form a "master curve," when G' and G'' data reduction involves a time equivalent shift factor. This may be either a temperature shift or molecular weight shift; for the latter the MWD and the degree of long branching of the samples must be similar. For example, the data from XL-0 which are located in the upper right portion of the Cole–Cole plot were obtained using either higher frequencies or lower temperatures, while those data located in the lower moduli region were obtained using either lower frequencies or higher temperatures.

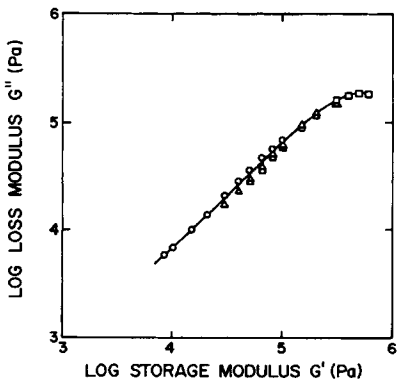

Fig. 9. Modified Cole–Cole plot for XL-4 showing inapplicability of time–temperature superposition when sample possesses extensive, long branching. (—) Approximate master curve; (○) 230°C; (△) 125°C; (□) 80°C.

TABLE III
GPC Measurements of EPM M_w Series[a]

Sample	M_n (10^4)	M_w (10^5)	M_z (10^5)	M_w/M_n	M_v (10^5)
A	4.92	1.13	2.29	2.29	1.02
B	5.42	1.35	3.53	2.49	1.20
C	6.15	1.56	3.34	2.53	1.39
D	6.09	1.70	6.27	2.80	1.46

[a] Symbols M_n, M_w, M_z, and M_v describe relative hydrodynamic size, i.e., molecular weight averages are not corrected for branching.

In order to explore the effect of an M_w shift on the Cole–Cole plot, four additional EPM samples having linear chains were selected and characterized. The composition, structure and MWD of these samples were similar to those of XL-0. The sample designation and GPC data are tabulated in Table III. The viscoelastic property measurements were performed in a manner similar to that previously discussed except that the eccentric rotating disc mode of operation was employed. The G', G'', and $|\eta^*|$ data were corrected for machine compliance contributions.[37]

As a point of reference, the $|\eta^*|$ curves for the four samples are presented with that of XL-0 in Figure 10. The relative magnitudes of $|\eta^*|$, especially at low frequency, reflects relative differences in M_w among the samples. As shown, the $|\eta^*|$ data of XL-0 falls between those of sample B and sample C. Close examination of the M_w data (Tables II and III) ranks the M_w of XL-0 between those of sample A and sample B. These observations suggest that a slight change occurred in the GPC calibration between the sets of measurements shown respectively in Table II and Table III. However, since the M_w/M_n remain relatively constant among these samples, this is not expected to alter the foregoing conclusions regarding the formation of a master curve. The G' and G'' data of these samples are presented in the form of the logarithmic Cole–Cole plot (Fig. 11). The data of all five samples are reduced to a single Cole–Cole plot master curve. The formation of a single Cole–Cole plot master curve indicates that an M_w change has no effect on the Cole–Cole plot. Specifically, this technique can

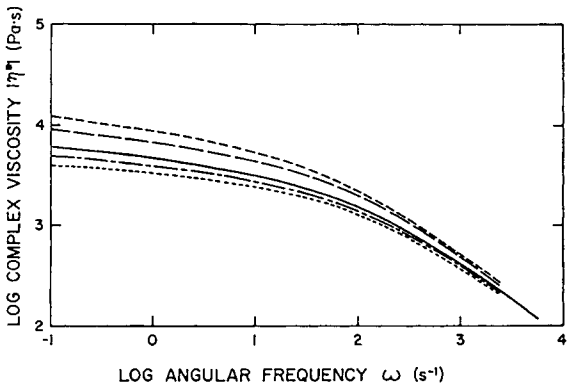

Fig. 10. Effect of variation in M_w on the complex viscosity master curves at 230°C. (- - -) A; (— - —) B; (- -) C; (- - - -) D; (—) XL-0.

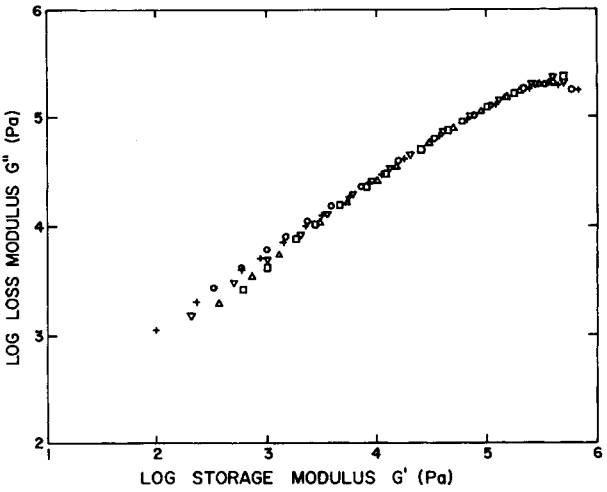

Fig. 11. Reduction of G' and G'' data to a unique molecular weight independent Cole–Cole master curve. (○) A; (△) B; (▽) C; (□) D; (+) XL-0.

be used to verify that samples possess variations only in M_w, if their dynamic properties form a single Cole–Cole plot.

The viscoelastic properties of the nearly monodispersed, linear, and star-branched polystyrene[12] and polybutadiene[13] model polymers, when examined with the modified Cole–Cole plot, display features which are consistent with the results of this study. In general, a single, molecular weight independent Cole–Cole plot is formed for each linear polymer species type and the introduction of branching shifts the Cole–Cole plot to higher values of G' at constant values of G''. A more detailed examination of these data will be presented at a later date.

In addition to variations in molecular architecture, the modified Cole–Cole plot can reveal variations in morphology, which produce different relaxation modes for molecular mobility. The utility of this technique is demonstrated in Figure 12 which shows the modified Cole–Cole plots of a polyvinyl chloride (PVC) homopolymer which was characterized at several temperatures. The G'

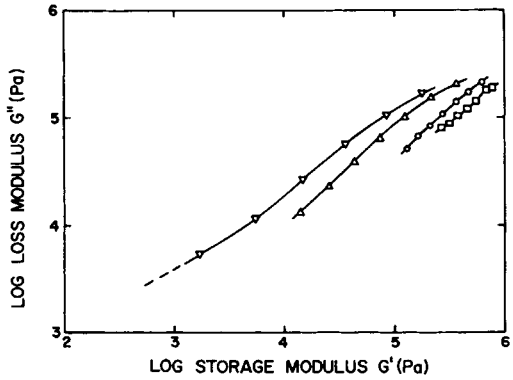

Fig. 12. Modified Cole–Cole plot showing the effects of temperature dependent variations in PVC morphology. (□) 175°C; (○) 190°C; (△) 210°C; (▽) 230°C.

and G'' measurements at each temperature were performed over the frequency range of 10^{-1}–10^{2} rad/s. As shown, separate Cole–Cole plots were formed by the data at each temperature, reflecting the temperature dependent change in sample morphology. As temperature increases, certain restrictions to molecular mobility are eliminated by the melting of crystalline domains, resulting in behavior that approaches that of a molecularly linear, amorphous polymer. Complete melting (in the absence of thermal degradation) can be ascertained if the dynamic data obtained at two different temperatures form a single modified Cole–Cole plot. For the case of the PVC sample, complete melting has not occurred at 210°C. Testing at temperatures greater than 230°C is required to assess complete melting at 230°C.

CONCLUSIONS

Recently, significant progress have been made in elucidating the effects of molecular architecture upon the rheological behavior of certain model polymer systems which contain well-defined branch frequency, branch length, and narrow MWD. However, the molecular architecture and hence the viscoelastic properties of many commercial elastomers are not well represented by these model systems. For example, the branching distribution in commercial elastomers is very complex and almost impossible to define precisely. Yet, these polymers manifest a common rheological response in processing, behaving as if they contain pseudocrosslinks. In viscoelastic characterization they seldom display frequency-independent, Newtonian viscosity or terminal flow behavior. Many commercial systems characteristically possess rubbery plateau-to-flow transition regions, encompassing many decades of deformation rate, over which the relative contributions of the G' and G'' remain essentially constant, even though both may vary by as much as three to four decades in magnitude. The viscoelastic properties of some elastomers have shown no regions of G'' dominated behavior over extensive ranges of frequencies, i.e., no G'–G'' crossovers were observed.[32] These variations in viscoelastic behavior are the manifestations of the broad MWD and long branching present in commercial elastomers.

In this work branch structures, which, based upon viscoelastic behavior, closely simulate those of commercial elastomers, were prepared. With these model polymers a method was developed to use viscoelastic properties for assessing variations in molecular architecture. The method recognizes the fact that the relative value of G' over that of G'' at low frequencies is affected by MWD and more significantly by the presence of long branching. Specifically, the method involves the use of a modified Cole–Cole plot for presentation and analysis of samples molecular characteristics. The practical use of the modified Cole–Cole plot has been demonstrated for the following three examples. When there is a difference in the degree of long branching, each sample gives a unique G'–G'' Cole–Cole plot. With many commercial elastomers, increasing the degree of long branching also results in broadening of MWD. The effect of variations in MWD, in the absence of architectural variations, upon the Cole–Cole plot remains for future study.

When both MWD and the degree of long branching remain approximately the same, the G' and G'' data form a molecular weight independent Cole–Cole master curve. The curve is considered to be a unique expression for a "family" of polymer-types. Such a family of polymers may be commercially desirable products which vary only in molecular weight.

Additionally, the modified Cole–Cole plot provides a sensitive technique for assessing differences in sample morphology such as degree of crystallinity.

Part of this investigation was performed in support of Epcar® EPDM which has since been acquired by Polysar Incorporated, Akron, Ohio. The authors are grateful to the B. F. Goodrich Chemical Group and Polysar Incorporated for permission to publish this paper. The GPC characterizations were provided by D. J. Harmon of B. F. Goodrich.

References

1. P. A. Small, *Adv. Polym. Sci.*, **18,** 1 (1975).
2. W. W. Graessley, *Acc. Chem. Res.*, **10,** 332 (1977).
3. J. D. Ferry, *Viscoelastic Properties of Polymers*, 2nd ed., Wiley, New York, 1970, p. 268.
4. G. Kraus and J. T. Gruver, *J. Appl. Polym. Sci.*, **9,** 739 (1965).
5. Ref. 3, p. 292.
6. N. Nakajima and P. S. L. Wong, *Trans. Soc. Rheol.*, **9**(1), 3 (1965); N. Nakajima, *Proc. Fifth Int. Cong. Rheol.*, **4,** 295 (1970).
7. R. P. Chartoff and B. Maxwell, *Polym. Eng. Sci.*, **9,** 159 (1969).
8. J. E. Guillet, R. L. Combs, D. F. Slonaker, D. A. Weemes, and H. W. Coover, Jr., *J. Appl. Polym. Sci.*, **8,** 757 (1965).
9. D. P. Thomas and R. S. Hagan, *Polym. Eng. Sci.*, **9,** 164 (1969).
10. C. D. Han and C. A. Villamizar, *J. Appl. Polym. Sci.*, **22,** 1677 (1978).
11. N. Nakajima and E. R. Harrell, *Rubber Chem. Technol.*, **53,** 14 (1980).
12. T. Masuda, Y. Ohta, and S. Onogi, *Macromolecules*, **4,** 763 (1971).
13. W. E. Rochefort, G. C. Smith, H. Rachapudy, V. R. Raju, and W. W. Graessley, *J. Polym. Sci., Polym. Phys. Ed.*, **17,** 1197 (1979).
14. T. Fujimoto, H. Narukawa, and M. Nagasawa, *Macromolecules*, **3,** 57 (1970).
15. T. Masuda, Y. Nakagawa, Y. Ohta, and S. Onogi, *Polym. J.*, **3,** 92 (1972).
16. G. Kraus and J. T. Gruver, *J. Polym. Sci., Part A*, **3,** 105 (1965).
17. H. Rachapudy, G. G. Smith, V. R. Raju, and W. W. Graessley, *J. Polym. Sci., Polym. Phys. Ed.*, **17,** 1211 (1979).
18. V. R. Raju, H. Rachapudy, and W. W. Graessley, *J. Polym. Sci., Polym. Phys. Ed.*, **17,** 1223 (1979).
19. N. Nakajima, Proceedings of the 7th International Congress on Rheology, Gothenburg, Sweden, August 23–26, 1976, p. 450.
20. N. Nakajima, *Polym. Eng. Sci.*, **19,** 215 (1979).
21. J. E. Guillet, R. L. Combs, D. F. Slonaker, D. A. Weemes, and H. W. Coover, Jr., *J. Appl. Polym. Sci.*, **9,** 767 (1965).
22. N. Nakajima, C. F. Stark, and R. D. Hoffman, *Trans. Soc. Rheol.*, **15,** 647 (1971).
23. N. Nakajima and E. R. Harrell, *J. Rheol.*, **26,** 427 (1982).
24. V. L. Folt, *Rubber Chem. Technol.*, **42,** 1294 (1969).
25. V. L. Folt, private communication, 1976.
26. N. Nakajima, E. R. Harrell, and D. A. Seil, *Rubber Chem. Technol.*, **55,** 456 (1982).
27. Technical Data Bulletin ORC-201C, Hercules Inc., Wilmington, Del.
28. F. P. Baldwin and G. Ver Strate, *Rubber Chem. Technol.*, **45,** 769 (1972).
29. J. R. Dunn, *Rubber Chem. Technol.*, **51,** 686 (1978).
30. W. W. Graessley and S. F. Edwards, *Polymer*, **22,** 1329 (1981).
31. R. Sabia, *J. Appl. Polym. Sci.*, **8,** 1651 (1964).
32. N. Nakajima, E. R. Harrell, and E. A. Collins, *Rubber Chem. Technol.*, **50,** 99 (1977).
33. K. S. Cole and R. H. Cole, *J. Chem. Phys.*, **9,** 341 (1941).
34. H. Leaderman, Proceedings of the 2nd International Congress on Rheology, Oxford, 1953, p. 203.
35. W. W. Graessley and J. Roovers, *Macromolecules*, **12,** 959 (1979).
36. S. V. Kanakkanatt, *J. Cell. Plast.*, **9**(1), 54 (1973).
37. C. W. Macosko and W. M. Davis, *Rheol. Acta*, **13,** 814 (1974).

Received June 23, 1983
Accepted September 15, 1983